Enhancing GNSS Positioning with 3D Mapping

Mounir Adjrad, Paul D Groves and Claire Ellul
University College London
London, United Kingdom
mounir.adjrad@ucl.ac.uk

***Abstract*— The number of global navigation satellite systems (GNSS) signals that can be received in dense urban areas has increased through the availability of multiple satellite constellations and high sensitivity receivers. However, in these constrained environments, the blockage and reflection of many of the signals by buildings and other obstacles means that poor positioning accuracy remains a problem that needs to be solved. Currently, no single positioning technology can cost effectively achieve reliable real-time metres-level positioning in dense urban areas. In response to these performance requirements, a concept known as intelligent urban positioning (IUP) has been proposed whereby multi-constellation GNSS is combined with three-dimensional mapping enabling techniques such as height aiding, non-line-of-sight (NLOS) detection and shadow matching. This paper demonstrates how conventional ranging-based GNSS positioning in dense urban areas can be enhanced using fully integrated and automated terrain height aiding exploiting data from 3D mapping. Using GPS and GLONASS data collected in London, it is shown that terrain height aiding can improve the single-epoch horizontal positioning accuracy by 43%. The paper also summarises UCL's plans for a full implementation of the IUP concept under the Intelligent Positioning in Cities project.**

Keywords- Multi-constellation GNSS, Intelligent Urban Positioning, Height Aiding, 3D Mapping

I. INTRODUCTION

Improving poor positioning accuracy in dense urban will unlock the potential for a host of new positioning applications such as navigation for the visually impaired, tracking people with chronic medical conditions and emergency caller location. For these latter applications, it is important to determine which side of the street a pedestrian is on and which building they are in front of. This is also useful for guiding visitors, meeting friends and business associates and location-based advertising, while augmented reality relies on knowing where the user is. Similarly, to make best use of the space in cities, sustainable transport requires advanced lane control systems for vehicles and advanced railway signaling systems, both of which require accurate positioning. With the emergence of citizen science, low-cost GPS-enabled devices to measure noise and pollution are becoming prevalent. As these measurements vary greatly across a street, accurate positioning is required to interpret the results. However, real-time positioning accuracy in cities is currently limited to 10-50m [1].

The Global Positioning System (GPS) provides metres-level positioning in open environments, but the accuracy and reliability in urban areas is poor because buildings block, attenuate, reflect and diffract radio signals. This has conventionally been a major hindrance to positioning, with errors of tens of metres common and often no position solution available at all [2]. Using the new GNSS constellations (GLONASS and, in future, Galileo and Compass) in addition to GPS dramatically increases the number of usable satellites. This improves the availability of a position solution in urban areas, but not the accuracy [3].

One way of improving positioning performance is to integrate GNSS with dead reckoning (DR) sensors, such as low-cost inertial sensors and car odometers [4], [5]. DR sensors measure change in position, so require a good GNSS position solution for initialisation. Following this, their positioning errors increase over time, so they are only useful for bridging short gaps in GNSS coverage. Furthermore, it can be difficult to determine the direction of travel in urban areas due to man-made magnetic fields disrupting magnetic compasses [6]. Map matching can be used to stop the position solution drifting off the street, but it cannot determine the position within the street [7].

Another approach is to use other widely available radio signals, such as eLoran, phone signals, Wi-Fi, television and broadcast radio [8]–[11]. However, these typically suffer from the same propagation errors as GNSS in urban environments so do not offer better accuracy. Metre-level accuracy can be achieved using techniques such as ultrawideband and bluetooth low energy [4]. However, these require installation of a dense network of base stations, which is far too expensive for most urban positioning applications.

The robotics community has conducted extensive research into visual navigation, much of it indoors. However, outdoor environments are much more challenging, with a need to collect reference data under many different lighting conditions [12] and filter out moving vehicles and pedestrians [13]. Furthermore, cameras are not practical for every application needing better urban positioning. Laser-based techniques have also been demonstrated [14] but are currently too expensive for most urban positioning applications.

Reliable meters-level positioning in dense urban areas is almost impossible to achieve cost-effectively using a single method. To achieve this goal, a paradigm shift is needed. Instead of designing a single-technology navigation or positioning system, we need to use as much information as we can cost-effectively obtain from many different sources in order to determine the best possible navigation solution in terms of both accuracy and reliability.

This new approach to navigation and real-time positioning in challenging environments requires many new lines of research to be pursued [15]. These include:

- How to integrate many different navigation and positioning technologies when the necessary expertise is spread across multiple organisations [16];
- How to adapt a multisensor navigation system in real-time to changes in the environmental and behavioural context to maintain an optimal solution [17];
- How to obtain more information for positioning by making use of new features of the environment [18];
- How to use 3D mapping to improve the performance of existing positioning technologies, such as GNSS, in dense urban areas.

The final item is the subject of the present paper. Intelligent urban positioning (IUP) aims to achieve a step change in the performance of real-time GNSS positioning in dense urban areas by combining three key ingredients [19]:

- Multi-constellation GNSS;
- New techniques for detection of non-line-of-sight (NLOS) signal propagation; and
- Three-dimensional mapping.

Making use of the signals from all visible GNSS satellites significantly increases the amount of information available to compute a position solution from. It also provides the flexibility to select which signals to use and which to discard. NLOS signals are received only via reflected surfaces and can contribute large ranging errors. If these signals can be identified and excluded [20], [21], the accuracy of conventional GNSS positioning may be substantially improved. Therefore, multi-constellation GNSS and effective NLOS detection are both critical components of any initiative to improve GNSS positioning accuracy in challenging urban environments.

There are at least three ways in which 3D mapping can be used to enhance GNSS positioning: detection and mitigation of NLOS reception, shadow matching and height aiding. A full IUP implementation would incorporate all three of these techniques and could also use conventional map matching [19].

A number of research groups have shown that 3D city models can be used to mitigate the effects of NLOS GNSS signal reception, a major source of error in dense urban areas. The 3D model can be used to predict which signals are NLOS and exclude these from the position solution [22], [23]. Using the 3D model to correct the NLOS ranging errors takes this a stage further [24], [25]. Multipath interference can also be predicted using a 3D city model, though correction is impractical. A limitation of current NLOS detection and mitigation techniques is that they either rely on prior knowledge of position or are highly computationally intensive. The challenge is therefore to develop a computationally efficient NLOS mitigation technique that can cope with position uncertainties of 10s of metres.

The second way of aiding GNSS using 3D mapping is shadow matching. This is a new technique that determines position by comparing the measured signal availability and strength with predictions made using a 3D city model [26]. It is designed to be used alongside conventional ranging-based GNSS positioning in dense urban areas in order to improve the cross-street accuracy. Since 2011, UCL and other research groups have demonstrated shadow matching experimentally, using both single and multiple epochs of GNSS data [27]–[30]. Cross-street positions within a few meters have been achieved in environments where the error in the conventional GNSS position solution is tens of meters, enabling users to determine which side of the street they're on. Shadow matching has also been demonstrated in real time on an Android smartphone [31]. The challenge ahead is to improve shadow matching's reliability and integrate it with other navigation and positioning techniques, starting with conventional ranging-based GNSS.

This paper focuses primarily on the third use 3D mapping to aid GNSS, namely terrain height aiding. This is described in Section II, with the results achieved using GPS and GLONASS data collected in London described in Section III. Section IV then discusses the proposed development of a full IUP system under the Intelligent Positioning in Cities (IPC) project. Finally Section V summarizes the conclusions.

II. TERRAIN HEIGHT AIDING

As demonstrated in [4], a position solution may be computed from a set of pseudo-range measurements using least-squares estimation. This is given by

$$\hat{\mathbf{x}}^{+} = \hat{\mathbf{x}}^{-} + \left(\mathbf{H}_G^{e\,\mathrm{T}}\mathbf{W}_\rho\mathbf{H}_G^{e}\right)^{-1}\mathbf{H}_G^{e\,\mathrm{T}}\mathbf{W}_\rho(\tilde{\mathbf{z}} - \hat{\mathbf{z}}^{-}), \quad (1)$$

with $\hat{\mathbf{x}}^{+}$ representing the estimated state vector, comprising the position and time solution, $\hat{\mathbf{x}}^{-}$ is the predicted state vector, $\tilde{\mathbf{z}}$ is the measurement vector, $\hat{\mathbf{z}}^{-}$ is the vector of measurement prediction from $\hat{\mathbf{x}}^{-}$, $\mathbf{W}_\rho$ is the weighting matrix and $\mathbf{H}_G^{e}$ is the measurement matrix. A detailed definition of equation (1) is provided in [21]. The different weighting schemes considered are: conventional elevation-based weighting and C/N_0-based weighting. $\mathbf{W}_\rho$ is given by

$$\mathbf{W}_\rho = \begin{pmatrix} \sigma_{\rho_1}^{-2} & 0 & \cdots & 0 \\ 0 & \sigma_{\rho_2}^{-2} & \cdots & 0 \\ \vdots & \vdots & \ddots & \vdots \\ 0 & 0 & \cdots & \sigma_{\rho m}^{-2} \end{pmatrix}, \quad (2)$$

with the elements of $\mathbf{W}_\rho$ for the elevation-based weighting and C/N_0-based weighting are as defined in [21]. For the case without weighting, $\mathbf{W}_\rho$ is simply the identity matrix.

Many conventional maps, dedicated digital terrain models (DTMs) and digital elevation models (DEMs) and all 3D maps provide the terrain height. Land vehicle or pedestrian GNSS user equipment may be assumed to be at a fixed height above the terrain. Therefore, the approximate GNSS horizontal position solution may be used to obtain a height solution from the mapping data or a separate terrain height database. This may then be used as an extra ranging measurement within a GNSS positioning algorithm, a technique known as height aiding [32]. Typically, the height-aiding measurement is treated as a virtual transmitter at the centre of the Earth, the

range to which is equal to the (local) Earth radius plus the height (Figure 1.).

If the terrain within the search area is not flat, the range may vary over the uncertainty bounds of the approximate GNSS position solution. Height aiding is particularly useful in cases where there are insufficient direct-LOS signals to determine a position solution without using NLOS signals. Under good GNSS reception conditions, height aiding only improves vertical positioning. However preliminary tests have shown that in areas such as urban canyons, where the signal geometry is poor, it can also improve horizontal positioning.

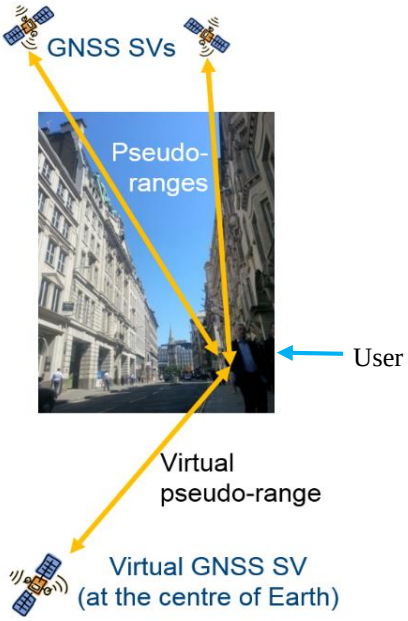

Figure 1. Terrain Height Aiding

Considering m GNSS range measurements, the height-aiding measurement forms the $m + 1^{th}$ component of the measurement vector $\mathbf{z}$. However, where this height is also used to calculate the predicted position, $\hat{\mathbf{r}}_{ea}^{e-}$, the height measurement innovation will be zero, i.e. $\hat{Z}_{m+1}^{-} = \bar{Z}_{m+1}$. The height aiding row of the measurement matrix is [21]

$$\mathbf{H}_{G,m+1}^{e} = (u_{ea,x}^{e} \quad u_{ea,y}^{e} \quad u_{ea,z}^{e} \quad 0 \quad 0), \qquad (3)$$

where $\mathbf{u}_{ea}^{e}$ is the unit vector describing the direction from the centre of the Earth to the predicted user position, given by

$$\mathbf{u}_{ea}^{e} \approx \frac{\hat{\mathbf{r}}_{ea}^{e-}}{|\hat{r}_{ea}^{e-}|}. \qquad (4)$$

Note that the columns of (3) corresponding to the receiver clock offset and the GLONASS-GPS interconstellation timing bias, where needed, are both zero. In the preliminary tests [21], height aiding measurements were simulated by taking the true value and adding a random error. Here we generate real height aiding measurements using only the GNSS measurements and a terrain height database.

Figure 2. summarises the iterative process of computing height aiding comprising three main steps:

1) Computing a position using pseudo-range measurements from all of the satellites tracked as described in equation (1) (using one of the weighting strategies mentioned before).
2) Following the computed position and coordinate transformation from WGS84 to the National Grid Easting and Northing coordinate system, a database containing terrain height information is then queried and the four DTM vertices surrounding the position solution are identified and extracted. These latter are then used in an interpolation process (as described in the next paragraphs) to extract a new height information corresponding to the computed position.
3) Following conversion of the height information into a virtual pseudo-range information, this latter is then included in the vector of measurements as described before and a new position solution is computed. The process iterated until the difference between the old and new position is lower than the DTM cell resolution.

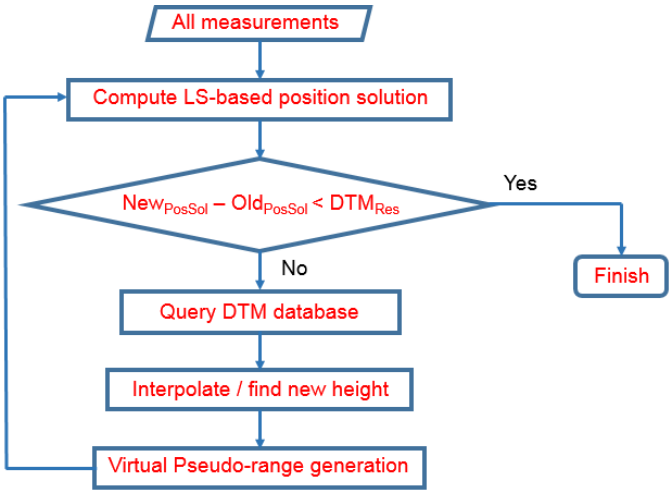

Figure 2. Terrain Height Aiding process

We examined the effect of different terrain resolutions, obtained from Ordnance Survey (OS) grid DTM 5 and DTM 50 (with 5m and 50m grid resolution, respectively, and both aving a 1.5m height information resolution) [33], on horizontal position and height accuracy for urban mobile positioning. Furthermore, the choice of interpolation algorithm for estimating heights from the DTM was investigated.

GNSS position solutions are unlikely to correspond to the grid points in any DTM. Therefore heights for aiding GNSS

positioning must be interpolated from surrounding points in the DTM. There are a variety of interpolation algorithms [34] (e.g. linear, bilinear, bicubic and biquintic). A higher order interpolant that takes account of the points beyond those immediately surrounding the position of interest, either directly or indirectly as slope estimates, will generally produce a better estimate than the bilinear algorithm. However, the more complex an interpolation algorithm is, the more computationally expensive it becomes, which may be a prohibitive overhead when computing GNSS positions using consumer devices such as smart phones. The first part of the work described here investigates how the choice of DTM and interpolation method affects the performance of the proposed positioning algorithm, in terms of horizontal position and height accuracy.

The study reported in [34] demonstrates that whether interpolating on mathematical surfaces or DTMs, irrespective of terrain complexity, the higher-order algorithms consistently outperform the simpler linear variant. For this study, two representative high-order interpolation algorithms, bicubic and biquintic, were implemented, as well as the more popular bilinear algorithm, often incorporated in desktop Geographic Information System (GIS) packages.

The most commonly used interpolation method for a regular grid is patchwise polynomial interpolation. The general form of this equation for surface representation is [34]

$$h = \sum_{i=0}^{m}\sum_{j=0}^{n} a_{ij} x^i y^j, \qquad (5)$$

where h is the height of an individual point with rectangular coordinates x and y, and $\{a_{ij}, i = 0, \cdots, m, j = 0, \cdots, n\}$ are the coefficients of the polynomial in (5).

Bilinear, Bicubic and biquintic interpolations makes use of the 4-term, 16-term and 36-term function, respectively, and the general form is derived by replacing in (5) with $m = n = 1$, $m = n = 3$, and $m = n = 5$, respectively. Since the coordinates of each grid vertex are known, the values of$\{a_{ij}, i = 0, \cdots, m, j = 0, \cdots, n\}$ can be determined from the set of simultaneous equations that are set up, one for each known point, or its derivative. For any given location with known coordinates, the corresponding elevation can be determined by a substitution into these equations.

For the bicubic interpolation, the 16 values used to derive the coefficients are the elevations at the four vertices of the grid cell, together with three derivatives. The first derivative with respect to x and y express the slope of the surface in the x and y directions, respectively, whilst the cross derivative represents the slope in both x and y. For the bicubic it is necessary to estimate the derivatives or slopes at the DEM vertices. Slope values will influence the shape of the interpolating surface function in a more valuable and accurate way than just using additional DEM vertices. To estimate these slopes from the grid elevations, we used finite difference approximations [35].

III. Experimental Results

The approach was tested on GPS and GLONASS data collected using a Leica GS15 survey-grade multi-constellation GNSS receiver in Central London. The first set of test data was collected near Moorgate underground station on 8th April 2011. There are three sites within the test data set, each occupied for about 38 minutes. Figure 3. shows an overview of the test sites. The truth was established using traditional surveying methods and is accurate at the cm-level. The second test data set was collected near Fenchurch Street station on 23rd July 2012. Overall 22 sites were occupied to cover a variety of environments. Each site was occupied for two periods of about 10 minutes approximately 3 hours apart. Figure 4. depicts an overview of the test sites. The truth was established to decimetre-level accuracy using a 3D city model with tape measurements from landmarks.

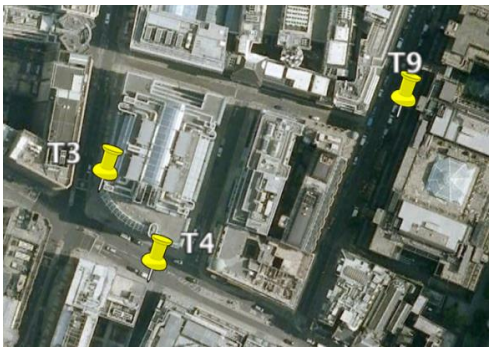

Figure 3. Locations of the Test Set 1 sites (Background Image © 2013 Bluesky © Google).

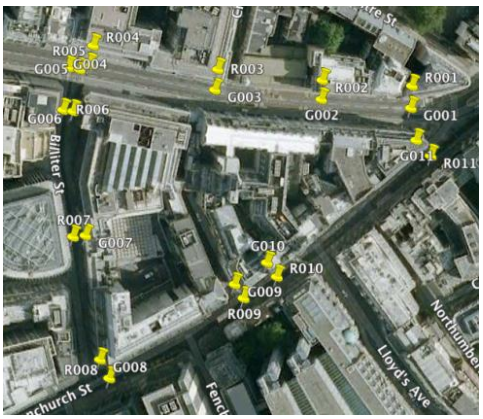

Figure 4. Locations of the Test Set 2 sites (Background Image © 2013 Bluesky © Google).

A number of combinations were tested as illustrated on Figure 5. . Figure 6. shows the horizontal and vertical RMS errors for test set 1, T3. No height aiding and automated height aiding, TDM 5, scenarios were tested. For both cases the C/N_0 weighting was considered. The figure clearly demonstrate the improvement of the accuracy in vertical and

horizontal directions when terrain height aiding is incorporated.

All combination results are given in TABLE I summarising the RMS horizontal and vertical position error with conventional GNSS positioning, simulated and automated terrain aiding for both C/N_0 and elevation based weighting and using OS DTM 5 and DTM 50. The results presented are those using the bicubic polynomial as it provided similar results to the biquintic polynomial interpolation and better overall performance than a bilinear interpolant. With C/N_0-based weighting, terrain height aiding improves the horizontal accuracy by 43% with DTM 5 and 31% with DTM 50.

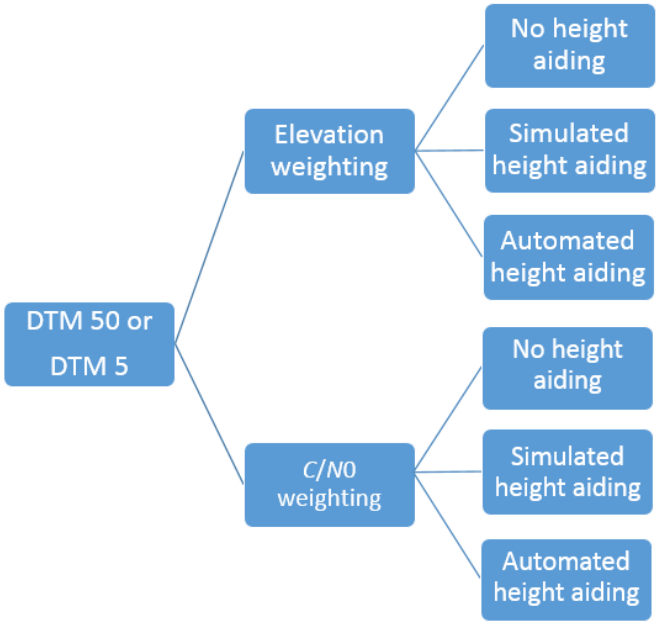

Figure 5. TESTED COMBINATIONS.

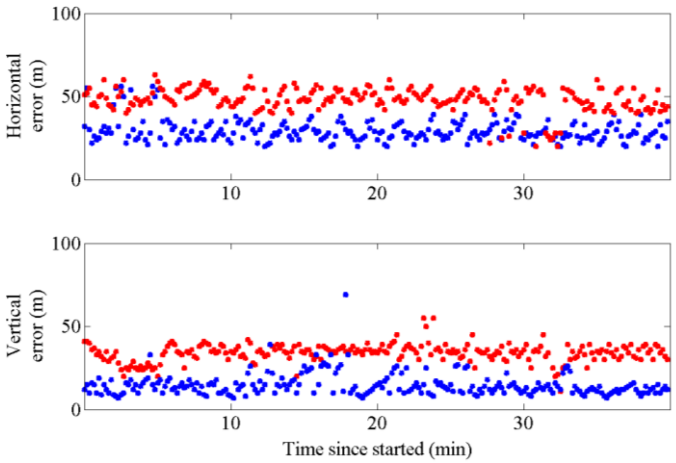

Figure 6. HORIZONTAL AND VERTICAL POSITIONING RMS ERRORS (ABSOLUTE VALUE) – TEST SET 1 (T3) FOR CASE WHERE NO HEIGHT AIDING IS APPLIED (RED) AND WHERE AUTOMATED HEIGHT AIDING IS INCORPORATED (BLUE) USING DTM 5 AND C/N_0 WEIGHTING..

TABLE I. POSITION ERRORS OBTAINED USING EACH METHOD

Positioning			**RMS Positioning Error (m)**	
Terrain Aiding		**Weighting**	**Horizontal**	**Vertical**
None		Elevation	50.1	53.9
		(C/N_0)	46.1	50.1
With simulated errors		Elevation	35.2	12.3
		(C/N_0)	32.1	13.5
bicubic interpolation and a 5m/50m grid spacing	DTM 50	Elevation	35.0	12.4
		(C/N_0)	32.0	13.4
	DTM 5	Elevation	30.2	10.6
		(C/N_0)	26.1	10.9

IV. INTELLIGENT URBAN POSITIONING

Following on from the work presented in Sections II and III and previous research at UCL [21], [27], [30], the Intelligent Positioning in Cities project will develop a full implementation of intelligent urban positioning. Two different approaches to NLOS mitigation using a 3D city model will be developed. The first will determine the average direct visibility of each GNSS signal over a position search area and combine this with UCL's consistency checking approach. The second method will adopt a hypothesis testing approach to ranging-based GNSS positioning in which an array of candidate positions are allocated likelihood scores.

The project will also integrate shadow matching with ranging-based GNSS positioning, including 3D-mapping-based NLOS mitigation and terrain height aiding. Conventional GNSS positioning is already used to initialize shadow matching. However, integration of the two position solutions has so far been limited to manually combining the cross-street shadow-matching solution with the along-street conventional GNSS solution [19]. Under IPC, a weighted average using error ellipses and a hypothesis-based integration approach will be investigated.

Considering the IUP process as a whole, one approach comprises the following six steps:

1) Compute an approximate conventional GNSS position solution using least-squares with basic outlier detection

2) Use predictions from the 3D city model and other information to identify potential NLOS and severely multipath-contaminated signals.
3) Compute an updated least-squares ranging-based GNSS position solution using terrain height aiding and excluding or downweighting those signals identified as NLOS or multipath contaminated in step 2.
4) Setup a search grid for shadow matching centred at the position solution from step 3 above.
5) Perform shadow matching, determining a score for each grid point and then producing a position solution from the scores.
6) Form an IUP position solution by combining the ranging-based position solution from step 3 with the shadow matching solution from step 5.

Within the IUP scope, many different factors will require further investigation. These include the building topology and reflectivity; the effect of human-body and vehicle shadowing; the quality of the user equipment; the available processing power and memory; and the number of GNSS signals available. Different versions of IUP are expected to evolve to meet the needs of different applications.

Of particular importance is the availability of 3D mapping. CityGML (the Open Geospatial Consortium's approved standard for storage and exchange of virtual 3D city models) [36] defines 3D city models as having varying levels of detail (LoD) [37], where LoD 0 is a digital terrain model, LoD1 is a block model without any roof structures (i.e. all the buildings have flat roofs) and LoD 2 is a city model having explicit roof structures and potentially associated texture. The process of extrusion ("growing") 2D topographic mapping data to a given height) means that it is now possible to very efficiently and cheaply create 3D LoD1 data by combining 2D mapping with height information (for example from Light Detection and Ranging , LiDaR, surveys. This can be achieved within standard Geographical Information Systems, resulting in rapid generation of city-wide dataset suitable for testing IUP. More detailed (and realistic) 3D buildings are also becoming available, either generated from individual Computer Aided Design (CAD) data, or from terrestrial or airborne LiDaR using dense point clouds to ensure detail is captured. Although this type of detailed model tends to be available mainly for urban, city centre, areas, these are in fact of great interest to IUP. These LoD 2 models may also be expensive, in particular where texture information is required. For both the flat roofs and more detailed 3D structures, the resulting 3D data is generally quite large in volume and complex in detail [38].

Finally, the project will develop context-determination algorithms [17] to identify, whether the user is in an indoor, urban or open environment so that the IUP algorithms are selected only when appropriate.

V. CONCLUSIONS

The ability of height aiding to improve GNSS positioning in dense urban areas using an automated iterative process has been assessed using data collected at multiple sites. Using a height aiding measurement from a 3D city model or separate terrain height database significantly improves single-epoch positioning accuracy, horizontally as well as vertically, due to the improved solution geometry. Horizontal accuracy is improved by 43% using a DTM with a 5m grid spacing and 31% with a 50m grid spacing.

In order achieve more accurate and reliable positioning in dense urban areas, the proposed implementation of intelligent urban positioning (IUP) has been briefly described. This combines multi-constellation GNSS with multiple techniques for detecting non-line-of-sight (NLOS) signal propagation and multiple techniques using three-dimensional mapping, including shadow matching.

ACKNOWLEDGEMENTS

This work is part of the Intelligent Positioning in Cities (IPC) Using GNSS and Enhanced 3D Mapping project, funded by the Engineering and Physical Sciences Research Council (EPSRC) (Grant EP/L018446/1). We also acknowledge the work of Dr Ziyi Jiang at UCL between 2011 and 2013, also funded by EPSRC, upon which this research builds.

REFERENCES

[1] Porretta, M., Milner, C., Ochieng, W., "User Requirements Document," EPSRC GAARDIAN Project, Imperial College London, 2011.

[2] Ballester-Gúrpide, Í., et al., "Future GNSS Constellation Performances inside Urban Environments," ION GPS 2000.

[3] Wang, L., Groves, P., Ziebart, M., "Multi-Constellation GNSS Performance Evaluation for Urban Canyons Using Large Virtual Reality City Models," J. Navigation, 65, 2012, 459─476. Also available from http://discovery.ucl.ac.uk/.

[4] Groves, P., Principles of GNSS, Inertial, and Multisensor Integrated Navigation Systems, 2nd Ed., Artech House, 2013.

[5] Zhao, L., Ochieng, W., Quddus, M., Noland, R., "An extended Kalman Filter algorithm for integrating GPS and low cost Dead Reckoning system data for vehicle performance and emissions monitoring". J. Navigation, 56, 2003, 257-275.

[6] Mather, C. , Groves, P., Carter, M., "A Man Motion Navigation System Using High Sensitivity GPS, MEMS IMU and Auxiliary Sensors," ION GNSS 2006.

[7] Ochieng, W., Quddus, M., Noland, R. "Integrated Positioning Algorithms for Transport Telematics Applications," ION GNSS 2004.

[8] Hide, C., et al., "Integrated GPS, LORAN-C and INS for Land Navigation Applications," ION GNSS 2006.

[9] Faragher, R., et al., "Opportunistic Radio SLAM for Indoor Navigation using Smartphone Sensors," IEEE/ION PLANS 2012.

[10] Rabinowitz, M., Spilker, J., "A New Positioning System Using Television Synchronization Signals," IEEE Trans. Broadcasting, 51, 2005, 51–61.

[11] Bensky, A., Wireless Positioning Technologies and Applications, Artech House, 2008.

[12] Churchill, W., Newman, P., "Continually Improving Large Scale Long Term Visual Navigation of a Vehicle in Dynamic Urban Environments," IEEE Intelligent Transportation Systems Conference 2012.

[13] McManus, C., et al., "Distraction Suppression for Vision-Based Pose Estimation at City Scales," IEEE Int. Conf. on Robotics and Automation, 2013.

[14] Baldwin, I., Newman, P., "Laser-only road-vehicle localization with dual 2D push-broom LIDARS and 3D priors," IEEE/RSJ Int. Conf. on Intelligent Robots and Systems, 2012.

[15] Groves, P. D.,Wang, L., Walter, D., Martin, H., Voutsis, K., Jiang, Z.,. The Four Key Challenges of Advanced Multisensor Navigation and Positioning, IEEE/ION PLANS 2014. Monterey, California. Also available from http://discovery.ucl.ac.uk/.

[16] Groves, P. D., "The Complexity Problem in Future Multisensor Navigation and Positioning Systems: A Modular Solution," Journal of Navigation, Vol. 67, 2014, pp. 311−206. Also available from http://discovery.ucl.ac.uk/.

[17] Groves, P.D., H. Martin, K. Voutsis, D. Walter, and L. Wang, "Context Detection, Categorization and Connectivity for Advanced Adaptive Integrated Navigation," Proc. ION GNSS+ 2013, Nashville, TN. Also available from http://discovery.ucl.ac.uk/.

[18] Walter, D. J., Groves, P. D., Mason, R. J., Harrison, J., Woodward, J. and Wright, P., "Novel Environmental Features for Robust Multisensor Navigation," Proc. ION GNSS+ 2013, 2013 Nashiville, TN. Also available from http://discovery.ucl.ac.uk/.

[19] Groves, P. D., Z. Jiang, L. Wang, and M. K. Ziebart, "Intelligent Urban Positioning using Multi-Constellation GNSS with 3D Mapping and NLOS Signal Detection," Proc. ION GNSS 2012, Nashville, TN. Also available from http://discovery.ucl.ac.uk/.

[20] Jiang Z., Groves P. D., "NLOS GPS signal detection using a dual-polarisation antenna," GPS Solutions 18(1):15-26, 2014. doi: 10.1007/s10291-012-0305-5. Also available from http://discovery.ucl.ac.uk/.

[21] Groves, P. D. and Jiang, Z. (2013). Height Aiding, C/N0 Weighting and Consistency Checking for GNSS NLOS and Multipath Mitigation in Urban Areas. Journal of Navigation, 66, 653−669. Also available from http://discovery.ucl.ac.uk/.

[22] Obst, M., et al."Urban Multipath Detection and mitigation with Dynamic 3D Maps for Reliable Land Vehicle Localization," IEEE/ION PLANS 2012.

[23] Peyraud, S., et al., "About Non-Line-Of-Sight Satellite Detection and Exclusion in a 3D Map-Aided Localization Algorithm," Sensors, 13, 2013, pp. 829-847.

[24] Bourdeau, A., Sahmoudi, M., "Tight Integration of GNSS and a 3D City Model for Robust Positioning in Urban Canyons," ION GNSS 2012.

[25] Betaille, D., et al. (2013). A New Modeling Based on Urban Trenches to Improve GNSS Positioning Quality of Service in Cities. IEEE Intelligent Transportation Systems Magazine, 5(3), 59−70.

[26] Groves, P. D. (2011). Shadow Matching: A New GNSS Positioning Technique for Urban Canyons. Journal of Navigation, 64, 417-430. Also available from http://discovery.ucl.ac.uk/.

[27] Wang, L., Groves, P. D. and Ziebart, M. K. (2013). GNSS Shadow Matching: Improving Urban Positioning Accuracy Using a 3D City Model with Optimized Visibility Prediction Scoring. NAVIGATION, 60, 195−207. (First published at ION GNSS 2012). Also available from http://discovery.ucl.ac.uk/.

[28] Yozevitch, R., Ben-Moshe, B. & Dvir, A. (2014). GNSS Accuracy Improvement Using Rapid Shadow Transitions. IEEE Transactions on Intelligent Transportation Systems, PP (99), 1-10.

[29] Isaacs, J. T., et al. (2014). Bayesian localization and mapping using GNSS SNR measurements. IEEE/ION PLANS 2014. Monterey, California.

[30] Wang, L., Groves, P. D. and Ziebart, M. K. (2015). Smartphone Shadow Matching for Better Cross-street GNSS Positioning in Urban Environments. Journal of Navigation, 68, doi 10.1017/S0373463.314000836. Also available from http://discovery.ucl.ac.uk/.

[31] Wang, L., Groves, P. D. and Ziebart, M. K. (2013). Urban Positioning on a Smartphone: Real-time Shadow Matching Using GNSS and 3D City Models. ION GNSS+ 2013. Nashville, Tennessee. Also available from http://discovery.ucl.ac.uk/.

[32] Amt, J. H. R., and Raquet, J. F. (2006). Positioning for Range-Based Land Navigation Systems Using Surface Topography. Proceedings of ION GNSS 2006, Fort Worth, TX.

[33] Ordnance Survey: https://www.ordnancesurvey.co.uk/

[34] Dorey, M., 2002. Digital elevation models for intervisibility analysis and visual impact assessment. Ph.D. Dissertation.

[35] Press, W. H., Teukolsky, S. A., Vetterling, W. T., Flannery, B. P., and Metcalf, M., 1996, Numerical Recipes – The Art of Scientific Computing (Cambridge: Cambridge University Press).

[36] OGC 2015, CityGML Standard, Open Geospatial Consortium (online) Available from: http://www.opengeospatial.org/standards/citygml [Accessed 3rd February 2015]

[37] Glander, T. and Dollner, J., 2008. Techniques for generalizing building geometry of complex virtual 3D city models. In: Advances in 3D Geoinformation Systems, Springer, pp. 381–400.

[38] Kolbe, T. H., Groger, G. and Pl¨ umer, L., 2005. CityGML: Interoperable access to 3D city models. In: Geo-information for disaster management, Springer, pp. 883–899.